ELSEVIER

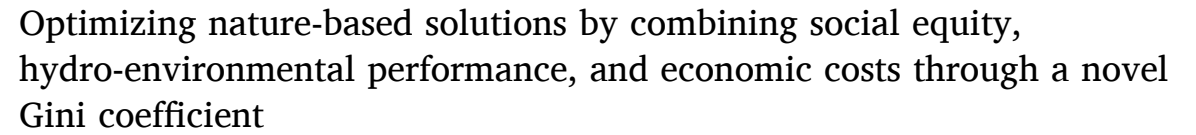
Contents lists available at ScienceDirect

Journal of Hydrology X

journal homepage: www.sciencedirect.com/journal/journal-of-hydrology-x



Research papers





C.V. Castro

Department of Civil Engineering, University of Illinois at Urbana-Champaign, Urbana, IL 61801, USA

ARTICLE INFO

Keywords: Area deprivation index (ADI) Gini coefficient Low impact development Multi-objective optimization Storm water management model (SWMM) Social equity

ABSTRACT

A robust multi-functional framework for widespread planning of nature-based solutions (NBS) must incorporate components of social equity and hydro-environmental performance in a cost-effective manner. NBS systems address stormwater mitigation by increasing on-site infiltration and evaporation through enhanced greenspace while also improving various components of societal well-being, such as physical health (e.g., heart disease, diabetes), mental health (e.g., post-traumatic stress disorder, depression), and social cohesion. However, current optimization tools for NBS systems rely on stormwater quantity abatement and, to a lesser extent, economic costs and environmental pollutant mitigation. Therefore, the objective of this study is to explore how NBS planning may be improved to maximize hydrological, environmental, and social co-benefits in an unequivocal and equitable manner. Here, a novel equity-based indexing framework is proposed to better understand how we might optimize social and physical functionalities of NBS systems as a function of transdisciplinary characteristics. Specifically, this study explores the spatial tradeoffs associated with NBS allocation by first optimizing a local watershed-scale model according to traditional metrics of stormwater efficacy (e.g., cost efficiency, hydrological runoff reduction, and pollutant load reduction) using SWMM modeling. The statistical dispersion of social health is then identified using the Area Deprivation Index (ADI), which is a high-resolution spatial account of socioeconomic disadvantages that have been linked to adverse health outcomes, according to United States census properties. As NBSs have been shown to mitigate various adverse health conditions through increased urban greening, this improved understanding of geospatial health characteristics may be leveraged to inform an explicit representation of social wellness within NBS planning frameworks. This study presents and demonstrates a novel framework for integrating hydro-environmental modeling, economic efficiency, and social health deprivation using a dimensionless Gini coefficient, which is intended to spur the positive connection of social and physical influences within robust NBS planning. Hydro-environmental risk (according to hydro-dynamic modeling) and social disparity (according to ADI distribution) are combined within a common measurement unit to capture variation across spatial domains and to optimize fair distribution across the study area. A comparison between traditional SWMM-based optimization and the proposed Gini-based framework reveals how the spatial allocation of NBSs within the watershed may be structured to address significantly more areas of social health deprivation while achieving similar hydro-environmental performance and cost-efficiency. The results of a case study for NBS planning in the White Oak Bayou watershed in Houston, Texas, USA revealed runoff volume reductions of 3.45% and 3.38%, pollutant load reductions of 11.15% and 11.28%, and ADI mitigation metrics of 16.84% and 35.32% for the SWMM-based and the Gini-based approaches, respectively, according to similar cost expenditures. As such, the proposed framework enables an analytical approach for balancing the spatial tradeoffs of overlapping human-water goals in NBS planning while maintaining hydroenvironmental robustness and economic efficiency.

1. Introduction

Renewed global mandates have encouraged a proliferation of nature-based solutions (NBSs) to deliver intersectoral functions of hydrological abatement, social well-being (e.g., mental and physical health, sense of place, vulnerability), and environmental health. According to UNEP (2019), widespread use of NBSs could help offset the negative consequences of climate change by addressing several United Nations Sustainable Development Goals concurrently, including improved social well-being, food security, ecosystem restoration, and hydrometeorological hazard reduction. When planning for such overlapping benefits, there will exist inherent tradeoffs between spatial priority and functionality that must be considered. As such, NBS optimization requires examining a range of transdisciplinary characteristics among human and physical domains to maximize the synergies between social equity and hydro-environmental performance (Frantzeskaki et al., 2019).

NBSs have evolved within the literature to encompass the urban drainage concepts of green infrastructure (GI), low-impact development (LID), best management practices (BMPs), sustainable urban drainage systems (SuDs), water-sensitive urban design (WSUD), and blue-green infrastructure (BGI) (Ruangpan et al., 2020). At the local scale (i.e., laboratory-, plot-, neighborhood-scale), NBS technologies have shown great promise in addressing stormwater abatement goals by improving peak runoff and attenuation, reducing hydrological flashiness, improving occurrence of combined sewer overflows, and reducing water contaminants (Boano et al., 2020; Jato-Espino et al., 2016; Kabisch et al., 2016; Loperfido et al., 2014; Ruangpan et al., 2020). However, NBSs are unlike traditional stormwater infrastructure due to regular human interaction with greenspaces. By increasing levels of urban vegetation, NBSs have been linked to a reduction in mortality (Gascon et al., 2016), cardiovascular diseases (Astell-Burt and Feng, 2021), diabetes, cancer (Mitchell and Popham, 2008), mental disorders (van den Berg et al., 2010), and respiratory diseases (Fuertes et al., 2014), which are disproportionately higher among racial and ethnic minorities and the socioeconomically disadvantaged (Luck et al., 2009). NBSs have also been shown to enhance social cohesion through improved recreational opportunities (Kaczynski and Henderson, 2007), reduced crime rates (Branas et al., 2011), increased land values (Vandermeulen et al., 2011), and enriched meeting spaces (de Vries et al., 2003). Consideration of social co-benefits has been increasingly valued throughout the NBS literature. For example Wolch et al. (2014) highlighted the need to consider social enhancement during urban planning of green infrastructure in addition to environmental sustainability. Studies have also shown that attitudes regarding NBSs are improved when stakeholders can readily identify how NBS solutions will benefit their locale according to both stormwater performance and societal improvement (Liu and Jensen, 2018; Sarabi et al., 2020; Wamsler et al., 2020). Therefore, NBS adoption depends partly on recognizing the unique spatial distribution of social characteristics in a given locale and identifying how the allocation of NBS features would address areas of highest impact.

Spatial characteristics of NBS co-benefits are often planned at the preliminary stage using data-overlay methods for defining hot-spots of multiple functions. For example, Meerow and Newell (2017) integrated social vulnerability, air quality, landscape connectivity, and urban heat island effects for NBS planning through visualization of geospatial characteristics, while flood-risk was estimated using historical flood events and a simplified runoff coefficient (i.e., using the Rational Method to estimate runoff from land use data). Similarly, the London Green Infrastructure Focus Map (GIFP) was designed for stakeholder prioritization of preferred NBS benefits (i.e., flood risk, water quality, air quality, social vulnerability, green space, and heat island) according to the perceived importance of each variable. Hydrologic factors were incorporated as pre-defined maps of areas that typically flood (i.e., 1% annual inundation boundary), which were superimposed into a geospatial map for holistic planning (GLA, 2018). Other studies have

employed spatial data overlay approaches for identifying areas of social vulnerability when prioritizing NBS allocation in urban planning (e.g., Heckert and Rosan, 2016; Jessup et al., 2021; La Rosa and Pappalardo, 2020). Wong and Montalto (2020) integrated social co-benefits with physical watershed performance through geospatial characteristics and agent-based modeling.

While such studies have highlighted the need to consider social characteristics at the early stages of NBS planning, they do not contain robust analysis of hydro-environmental performance. Conversely, twodimensional modeling programs are often used to assess NBS hydrodynamics for localized planning (e.g., SWMM, SUSTAIN, MIKE-URBAN), where numerous studies have been conducted to analyze hydrograph characteristics of NBS implementation with varying results regarding optimal performance (e.g., Huang et al., 2019; Jarden et al., 2016; Jato-Espino et al., 2016; Radinja et al., 2019; Zellner et al., 2016). Such high-resolution techniques are important in assessing NBS performance due to the unique mechanisms associated with interacting zones of vegetation, soil, and land surface in a water balance model (further detailed in SI Text S.1). As two-dimensional modeling is computationally-expensive, various optimization tools have been developed to simulate and compare allocation schemes for identifying the ideal placement of NBS features as a function of cost and performance (e.g., Lee et al., 2012; Macro et al., 2019; SFEI, 2018). Many studies have coupled the popular Nondominated Sorting Genetic Algorithm II (NSGA-II) with hydro-dynamic modeling to analyze the tradeoffs between NBS performance and cost (Alamdari and Sample, 2019; Giacomoni and Joseph, 2017; Krebs et al., 2013; Mani et al., 2019; Muleta and Boulos, 2007; Oraei Zare et al., 2012; Raei et al., 2019; Tao et al., 2014; Zhang et al., 2013).

While these decision-support tools have successfully combined high-resolution modeling with optimization techniques, they lack assessment of the unique spatial exposures of social characteristics that could benefit from NBS implementation. By relying on multi-functional data overlays *or* complex modelling tools, such planning may fail to allocate NBSs throughout space in a manner that fully espouses social needs while maintaining hydro-dynamic rigor (Kandakoglu et al., 2019). In this way, NBS plans may not realize the full locational benefits available, thus limiting their maximum potential to mitigate cross-cutting issues within the urban fabric.

Here, a novel equity-based indexing framework is proposed to better understand how we might optimize transdisciplinary characteristics of NBS systems. Specifically, this study explores the spatial tradeoffs associated with NBS allocation by first optimizing a local watershedscale model according to traditional metrics of performance (e.g., cost efficiency, hydrological runoff reduction, and pollutant load reduction) using SWMM software and NSGA-II optimization. The statistical dispersion of social health is then identified using the Area Deprivation Index (ADI), which is a high-resolution spatial account of socioeconomics disadvantages that have been linked to adverse health outcomes, according to United States census characteristics. The ADI is incorporated into the optimization scheme using a novel area-based Gini coefficient to combine the hydro-environmental performance of NBS siting with social characteristics across space. The Gini coefficient is a statistical representation of inequality across a population, commonly used within the social sciences to assess the degree of income equality between disparate locations (Gini, 1912). By extending the Gini coefficient to represent hydrological efficacy and social impact, this study provides a novel means for allocating NBSs according to both their physical performance and also the locational characteristics of persons that would be influenced by varying spatial arrangements. The proposed Gini-based framework provides a common, dimensionless measurement unit for capturing transdisciplinary variations across space to spur the positive connection of social and physical influences associated with NBS systems while maintaining hydro-dynamic rigor.

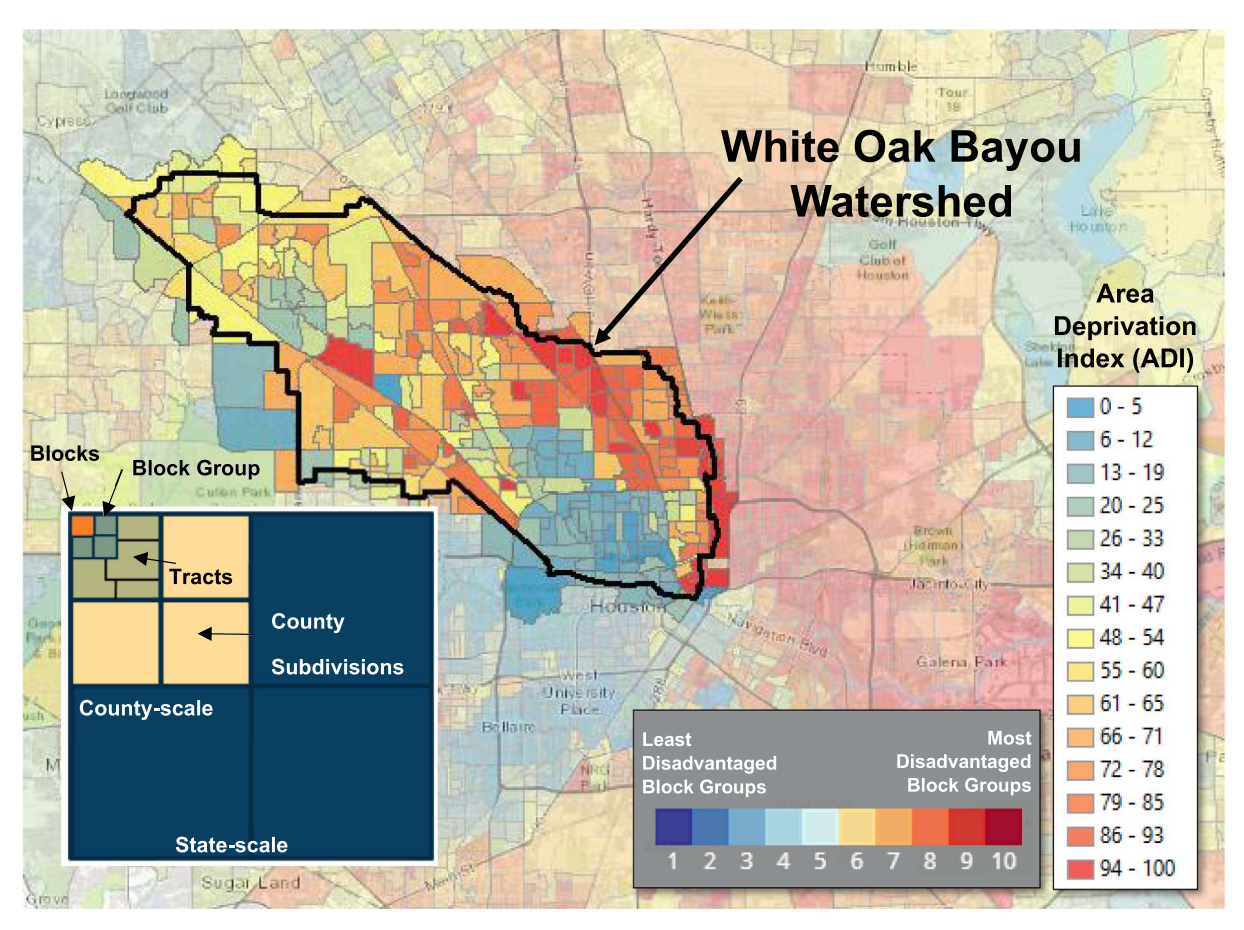


Fig. 1. Area deprivation index for the White Oak Bayou watershed.

2. Materials and methods

2.1. White Oak Bayou case study

The White Oak Bayou (WOB) in Houston, Texas, USA was chosen as the case study due to its history of flooding (Sipes and Zeve, 2012) and its potential for improving various metrics of social deprivation through enhanced levels of greenspace, including reduced morbidity and risk of disease, increased mental health of residents, and improved levels of environmental and economic prosperity (C40, 2017; Crompton, 2012). Current stormwater management within the study area is based on a 'worst-first' framework (Despart, 2019), where hydrological improvements are prioritized according to flood risk reduction and the number of persons benefited, irrespective of their socioeconomic conditions. Such frameworks do not address inherent vulnerabilities within the population served to consider human aspects, such as ability to recover from a storm or the reinforcing impacts of hydro-environmental hazards on social health. As such, the ADI is adopted as a spatial representation of social deprivation throughout the watershed to highlight areas of greatest potential health benefit when planning multi-functional NBSs.

2.2. Area deprivation index

The ADI was introduced in 2016 as a proxy indicator of socioeconomic status from census results that were curated to reflect risk factors associated with long-term health and social well-being (Knighton et al., 2016). The ADI has been used within the medical literature to measure social determinants that have been shown to influence public health issues, such as cancer rates (Kurani et al., 2020), hospital admissions (Hirshberg et al., 2019; Ingraham et al., 2021), asthma (Nkoy et al., 2018), obesity (Ludwig et al., 2011), diabetes (Addala et al., 2021),

mental health (Martikainen et al., 2004), and mortality (Chamberlain et al., 2020; Singh, 2003), each of which are positively impacted by NBS systems (van den Bosch and Ode Sang, 2017). The ADI merges characteristics of income, employment, education, and housing from the United States census to represent social disadvantage (Kind and Buckingham, 2018), which have been shown to collectively influence communal health (Link and Phelan, 1995).

An advantage of using the ADI for NBS planning, as opposed to other social indices, involves its highly granular geospatial scale. The ADI provides a unique measurement of social deprivation for each census block group within the United States. Other standard metrics of social vulnerability, such as the Center for Disease Control (CDC) Social Vulnerability Index (SoVI) (Flanagan et al., 2020), are delineated at the census tract-scale, thereby lacking spatial heterogeneity to assess key differences at the neighborhood-scale. [Note: Census tracts are subdivisions of counties encompassing approximately 4,000 residents within each bound. Block groups are subdivisions of census tracts encompassing approximately 250–550 housing units each, demarcated by local streets (Schlossberg, 2003).

The ADI for the study area was downloaded from the University of Wisconsin's Neighborhood Atlas for year 2019 (Kind and Buckingham, 2018). The weighted ADI values within each spatial unit are represented at the national-level by a percentile (1–100) and at the state-level by a decile (1–10), with lower values denoting greater disadvantage (University of Wisconsin School of Medicine and Public, 2019). For example, an ADI value of 1 on the national scale represents an area that is more disadvantaged than the remaining 99% of census blocks within the nation. At the state-scale, an ADI of 1 implies that the given census block is more disadvantaged than 90% of the other census blocks within that state. Here, the national-level ADI was used to depict spatial variation of social deprivation throughout the WOB watershed (Fig. 1).

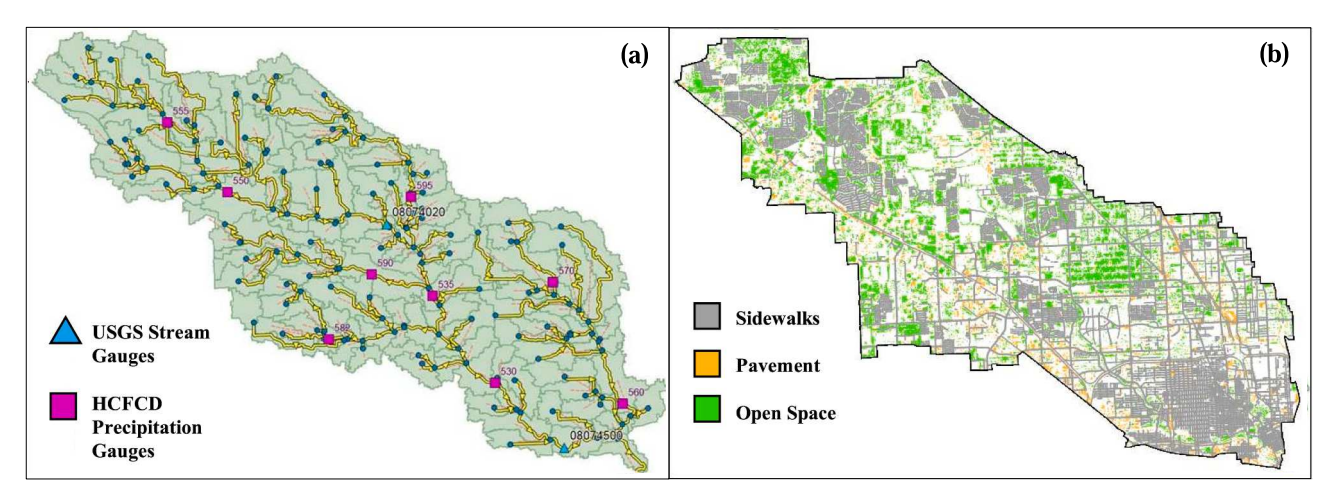


Fig. 2. (a) PCSWMM basin model, stream gauges, and precipitation gauges for WOB; (b) Geospatial siting of potential NBS locations in the WOB watershed.

2.3. Hydro-environmental SWMM model

2.3.1. Hydrological modeling

The basin model for the WOB watershed was initialized using the HMS-PrePro tool, which rapidly delineates a watershed into subcatchments according to the local terrain, connects hydrological topology in a format consistent with standard hydrological modeling software, and estimates common hydrological parameters to represent basin infiltration, runoff, and channelized flow routing (Castro and Maidment, 2020). The Green-Ampt method was used to represent infiltration losses within each subcatchment according to local empirical values used in FEMAeffective hydrology models for the WOB watershed (HCFCD, 2019) (initial content = 0.067, saturated content = 0.46, suction = 3.553 in., conductivity = 0.032 in./hour). The SWMM software routes overland flow to the subcatchment outlet using a property called the 'characteristic width', which is defined as the subcatchment area divided by the average maximum overland flow length (Rossman and Huber, 2016). The longest flow path for each subcatchment was calculated in HMS-PrePro according to 2018 LiDAR at 10-centimeter resolution (TNRIS, 2019). The time of concentration for each subcatchment was calculated using the TR-55 methodology for urban watersheds (USDA, 1986). Other principal inputs for modeling subcatchments in SWMM included average land use, impervious coverage, subcatchment area, and terrain slope, which were each estimated using HMS-PrePro.

PCSWMM version 7.4.3240 (Hamouz et al., 2020), which is a proprietary software designed as a user-friendly interface to the Environmental Protection Agency (EPA) SWMM program, was used to convert the preliminary basin into a SWMM model. To route flow through the watershed stream network, the PCSWMM Transect Tool was used to create average cross-sections for each system channel from the 2018 LiDAR elevation model (CHI, 2014). Design storm data for the Houston region was obtained from Barrett (2019) and COH (2019a) to represented the latest Atlas 14 precipitation frequency estimates in Texas, according to the National Oceanic and Atmospheric Administration (NOAA) (Perica et al., 2018). The rainfall intensity values for the Houston-area were used to develop intensity—duration frequency (IDF) curves in PCSWMM for varying annual exceedance probability (AEP) storm events (summarized in Table S.1).

2.3.2. Pollutant load modeling

The event mean concentration (EMC) method was used to estimate non-point water pollution within each subcatchment according to

$$EMC_i = \frac{\int C_i Q_i dt}{\int O_i dt},\tag{1}$$

where EMC_i is the event mean concentration, C_i is the standard con-

centration of a target pollutant, and Q_i is the runoff volume for each subcatchment, i, changing over simulation time t.

Local stormwater monitoring data was obtained from the National Stormwater Quality Database (NSQD), which contains public water quality metadata from over 9,000 runoff events for approximately 200 municipalities in the United States, including 41 monitoring stations within Harris County, Texas (Pitt et al., 2015). Since the GreenPlan-IT algorithm searches for the most cost-effective solution according to an individual pollutant type (further described in Section 2.4), total suspended solids (TSS) were chosen as the criteria pollutant due to the strong adsorption effects of TSS on other contaminants (Liu et al., 2019; Rossi et al., 2006). TSS concentrations were obtained for various land use types within the NSQD and averaged for each WOB subcatchment. The land use values in the WOB basin model were obtained from the 2016 National Land Cover Database (NLCD), which contains 16 unique land classifications based on the modified Anderson Level II scheme (Yang et al., 2018). The removal efficiency for each of the NBS features in this study were obtained from the 2020 International Stormwater BMP Database (Clary et al., 2020), summarized in Table S.2.

2.3.3. NBS water balance modeling

EPA's SWMM engine calculates the water balance for NBS-driven systems using a nonlinear reservoir model (Chen and Shubinski, 1971) according to a unique set of infiltration, storage, and evaporation properties that describe, on a per-unit-area basis, how NBS structures impact hydrological behavior (further described in SI Text S.1). Within NBS systems, the surface zone represents the ground surface, which stores excess inflow and generates outflow either overland or to an adjacent drainage system. The soil zone is comprised of an engineered soil mixture that allows water to percolate into the underlying zone, which may consist of rock and gravel for additional storage. The underdrain system conveys water out of the storage layer and into an engineered outlet. The three NBS features used in this case study (bioretention cells, porous pavement, and tree boxes) are summarized in Table S.3 as a function of their representative water balance layers. In the WOB case study, tree boxes were modeled as bioretention cells with no outflow drain. Various input parameters are also required within a SWMM model to describe the engineered design of local NBS features (e.g., conductivity rate, vegetation volume, clogging properties, surface roughness, etc.), which were obtained from the City of Houston design guidelines for low impact development (COH, 2019b) and summarized in Table S.4.

2.3.4. Calibration & validation

The hydrological basin parameters were calibrated to observed streamflow measurements from United States Geological Survey (USGS)

stream gauges #08074020 and #08074500 (USGS, 2021a, USGS, 2021b). One year of daily precipitation values were obtained from the Harris County Flood Warning System (HCFWS) precipitation gauges #530, #535, #550, #555, #560, #570, #582, #590, and #595 (HCFCD, 2021), encompassing the totality of the White Oak Bayou (Fig. 2a). The first six-months of precipitation data (October 2, 2020 -March 2, 2021) were used to calibrate the model, while the latter sixmonths of data (March 3, 2021 - August 2, 2021) were used to validate the model. The annual set of hydrographs for the basin model was disaggregated for wet weather conditions with a criterion of at least 500 cfs flow for a minimum of 4 consecutive hours, resulting in ten unique storm events for calibration and eight unique storm events for validation. The wet weather flow hydrographs were calibrated using the PCSWMM SRTC tool by selecting uncertainties for control parameters based on their data source and sensitivity gradient, per guidelines proposed by Choi and Ball (2002 and James (2003). The basin model was then simulated with the calibrated parameters and compared to observed streamflow to measure the goodness-of-fit using the integrated square error (ISE), further described in SI Text S.2. Model calibration and validation results are detailed in the supplementary materials, Tables S.5 – S.6 and Fig. S.2.

2.4. Spatial allocation optimization

The decision support tool GreenPlan-IT was used to optimize NBS siting within the calibrated model according to levels of runoff reduction, pollutant load abatement, and cost effectiveness (Wu et al., 2019) by coupling the NSGA-II algorithm with SWMM (SFEI, 2018). This optimization tool compares the performance of various NBS strategies to the baseline scenario, which represents watershed conditions prior to NBS implementation. Model performance is defined by three objectives: 1) minimizing the total relative cost expenditures for NBS implementation, 2) maximizing the reduction in hydrological runoff volume, and 3) maximizing abatement of pollutant loadings within the study area. The GreenPlan-IT package combines several unique tools that operate in succession to identify the optimal spatial allocation of NBS features within the study area, including:

- GIS-based Site Locator Tool (SLT): Merges spatial characteristics of NBS feature types with regional geospatial information to identify all possible NBS siting locations within the study area,
- 2) EPA SWMM Basin Model: Establishes baseline conditions for runoff and pollutant loadings throughout the study area and simulates proposed conditions according to unique NBS siting schemes, and
- 3) GreenPlan-IT Optimization Tool (GPOT): An executable file that runs through the user's command prompt to identify optimal combinations of NBS types within each catchment area according to a costbenefit analysis (where cost targets are defined by the user, and benefits are calculated using SWMM simulations to assess the reduction in stormwater runoff and pollutant loading over many NBS configurations).

The SLT was used to identify all potential locations of NBS features within the WOB watershed, as shown in Fig. 2b. Potential locations for bioretention cells, permeable pavement, and tree boxes were defined according to open space land use parcels, areas of existing pavement, and adjacent land near existing sidewalks, respectively. Corresponding data layers were obtained from the City of Houston GIS Data Hub (COH, 2021). Baseline flows and TSS loadings were quantified within the SWMM model for various design storm events, as described in Sections 2.3.1-2.3.2. The SLT output then served as a spatial constraint for the GPOT, which executed several thousand SWMM models according to unique spatial allocations of NBS features within the permissible areas (i.e., the shaded areas shown in Fig. 2b).

Relative cost estimates for the case study were obtained from the EPA National Stormwater Calculator (NSWC), which provides annual costs

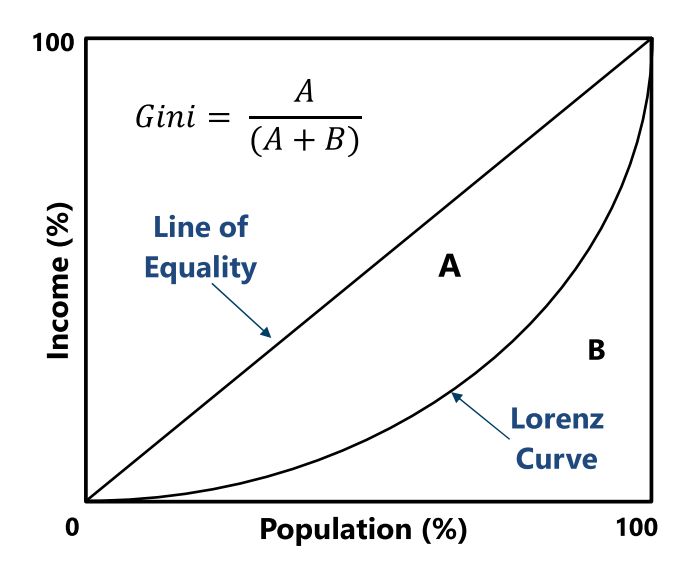


Fig. 3. Conceptual graph of Gini-based equality and Lorenz curve.

for NBS implementation and maintenance within unique geographical regions (CNT, 2009). At the time of study, the NSWC cost estimates for the Houston-area included: pervious pavement = \$8.68/SF, bioretention cells = \$6.07/SF, and tree planter boxes = \$9.46/SF (Bernagros et al., 2021). The GPOT used two input files to compare NBS scenarios with the baseline SWMM model. The first input file contained the total acreage, percent impervious coverage, and maximum number of NBS locations per subcatchment, as summarized in Table S.7. The second input file described average sizing parameters proposed by SFEI (2018), where bioretention cells, pervious pavements, and treeboxes were assigned uniform areas and widths of 500 SF by 20 FT, 5000 SF by 50 FT, and 60 SF by 6 FT, respectively.

The GPOT searches for the optimal solution among numerous possible scenarios by first modeling a random set of NBS placements and comparing their outputs for non-dominance according to the NSGA-II algorithm (Deb et al., 2002). Non-dominance occurs when a solution performs no worse than any other solution for all objectives (e.g., cost, runoff, and pollutant load efficiency) and also performs better than all other solutions within the cohort for at least one objective. This cohort (known as a generation) sorts each of the sub-routines within the series (known as a population) using the previous generation's non-dominant solutions and relative populations until the system either reaches a maximum number of simulations or until no further changes are observed. The GreenPlan-IT tool for the WOB case study used a threshold of 100 generations and 250 populations for a maximum of 25,000 unique configurations. The GPOT outputs were plotted as a function of cost (x-axis) and runoff/load reduction (y-axes) to assess the cost-efficiency of hydro-dynamic performance among many possible siting plans. The resulting graphs contained a set of all quasi-optimal solutions for NBS spatial allocation according to the targets on the plotted axes (known collectively as the Pareto set). Through the NSGA-II algorithm, the Pareto set converged to identify the optimal allocation of NBSs along a cost-efficiency curve, (also known as the Pareto curve or Pareto front), where no further improvements could be made through reallocation of NBS features (Wu et al., 2019).

2.5. Multi-objective Gini index

The Gini coefficient is a common index used in economics to describe the statistical dispersion of income and population within a sample group. In a perfectly equal society, the distribution of income (x-axis) would match the distribution of population (y-axis), known as the 'Line of Equality' in Fig. 3. In a more realistic scenario, the cumulative percentage of population versus household income often follows an

exponential distribution, called the Lorenz curve, which delineates state spaces A (e.g., the inequality gap) and B (e.g., the actual income distribution), described graphically by

$$Gini = \frac{A}{(A+B)},\tag{2}$$

where A represents the total area between the line of equality and the Lorenz curve distribution, and B represents the area between the Lorenz curve and the base axis.

A numerical form of the Gini coefficient (G_i) is given by

$$G_i = 1 - \sum_{i=1}^{I} (Y_i - Y_{i-1})(X_i + X_{i-1}), \tag{3}$$

where X_i is the cumulative percentage of the variable on the x-axis, and Y_i is the cumulative percentage of the variable on the y-axis, for data point i, from i = 1 to i = I total data points.

Gini values range from 0 to 1, where 0 indicates absolute equality, and 1 represents absolute inequality. Due to the popularity of the Gini coefficient to quickly identify statistical differences in distribution, studies have begun applying this economic concept to issues of energy appropriation (Jacobson et al., 2005; Saboohi, 2001), environmental inequity (Boyce et al., 2016; Heerink et al., 2001; White, 2007), water resources distribution (Cho and Lee, 2014; Du et al., 2021; Hu et al., 2016; Yan et al., 2018), flood drainage rights (Zhang et al., 2020), and other topics regarding allocation of limited natural resources (Josa and Aguado, 2020). In the environmental literature, recent applications have emerged to represent the Gini axes spatially using the area-based Gini ("AR-Gini"), which compares social metrics, calculated on an area basis, to a distributed good, calculated on a resource basis (Druckman and Jackson, 2008). An example of using the AR-Gini coefficient beyond the traditional scope of economic wealth disparity is given by Sun et al. (2010), where wastewater discharge permitting was optimized using the Gini index and a multi-criteria assessment of land, population, income, and environmental capacity. In this study, the conflict between wastewater efficiency and social equality was bridged by balancing tradeoffs between various policy-making goals amidst limited resources (Sun et al., 2010).

The AR-Gini is extended here to consider the spatial patterns of NBS allocation and performance with the distribution of social characteristics. The cumulative area of NBS allocation is plotted on the Gini y-axis as a proportion of subcatchment area normalized on a scale from 0 to 100. Unique evaluation indicators (e.g., stormwater runoff, stormwater quality, and social equity) are then plotted on the Gini x-axes, such that each potential NBS scheme contains three different Gini indices. Hydrological efficiency is represented as the percent difference of stormwater runoff volume between baseline and optimized conditions as a function of cost. Environmental efficiency is described as the percent difference of pollutant load abatement between baseline and optimized conditions on the basis of cost. Social equity is a function of the average neighborhood disadvantage (i.e., ADI score) over the weighted area of NBS allocation within each subcatchment. The individual Gini indices are combined to derive a single, dimensionless coefficient for transdisciplinary planning. A high composite Gini coefficient would suggest that the distribution of NBSs is skewed toward either hydro/environmental efficiency or social equity and does not maximize spatial allocation according to all three characteristics. A low composite Gini coefficient would reveal an ideal state space of NBS distribution that achieves maximum hydro-environmental performance while siting NBS features in locations with the greatest potential for social health improvement.

The following equations are used in deriving the individual Gini indices:

$$\omega_i = \sum_{j=1}^n z_{ji} A_j,\tag{4}$$

where ω_i is the allocation of NBS area per subcatchment i, n is number of

unique NBS feature types j = bioretention cells, porous pavements, or tree boxes, z is the number NBSs per subcatchment, A_j is the area of each NBS feature type (A_j : bioretention cells = 500 SF, porous pavements = 5,000 SF, tree boxes = 60 SF),

$$\eta_{(H|E)i} = \frac{\left(\frac{a_i - b_i}{a_i}\right) * 100}{\omega_i c_i},\tag{5}$$

where η_i is the percent efficiency of hydrologic (H) and environmental (E) improvement between the baseline model, a, and the optimized model, b for each subcatchment i, normalized by the cost of NBS features, c_j ($c_j = \$6.07/\text{SF}$, \$8.68/SF, \$9.46/SF for j = bioretention cells, porous pavements, and tree boxes, respectively), [Note: a and b represent the total stormwater runoff volume (V_R , in million gallons) for hydrologic efficiency (H) and the total pollutant load runoff (TSS, in lbs) for environmental efficiency (E), obtained from SWMM modeling], and

$$\mu_{si} = \frac{ADI_i}{\sum_{i=1}^m \omega_i},\tag{6}$$

where μ_{si} is the percent of NBSs sited within areas of high ADI, normalized by subcatchments area, ω_i , for all subcatchments m, and the social inequality within the subcatchment is measured by the average spatial ADI score within each subcatchment i.

To eliminate differences in measurement units and magnitudes among evaluation choices, each indicator is normalized on a scale of 0 to 100, per

$$x' = \frac{x - x_{min}}{x_{max} - x_{min}} *100, \tag{7}$$

where x' is the normalized value of each x = hydrologic efficiency (η_{Hi}), environmental efficiency (η_{Fi}), and social equity (μ_{si}).

Consequently, the sum of the normalization series for each Lorenz curve axis is 100. The composite Gini coefficient is then calculated by:

$$Y_i = Y_{i-1} + \frac{\omega_i'}{\sum_{i=1}^m A_i} *100,$$
(8)

$$X_i = X_{i-1} + \left(\frac{\eta_{Hi}}{\sum_{i=1}^{m} \eta_{Hi}}\right) * 100,$$
 (9a)

$$X_i = X_{i-1} + \left(\frac{\eta_{Ei}}{\sum_{i=1}^{m} \eta_{Ei}}\right) * 100,$$
 (9b)

$$X_i = X_{i-1} + \left(\frac{\mu_{si}'}{\sum_{i=1}^{m} \mu_{si}'}\right) * 100,$$
 (9c)

and

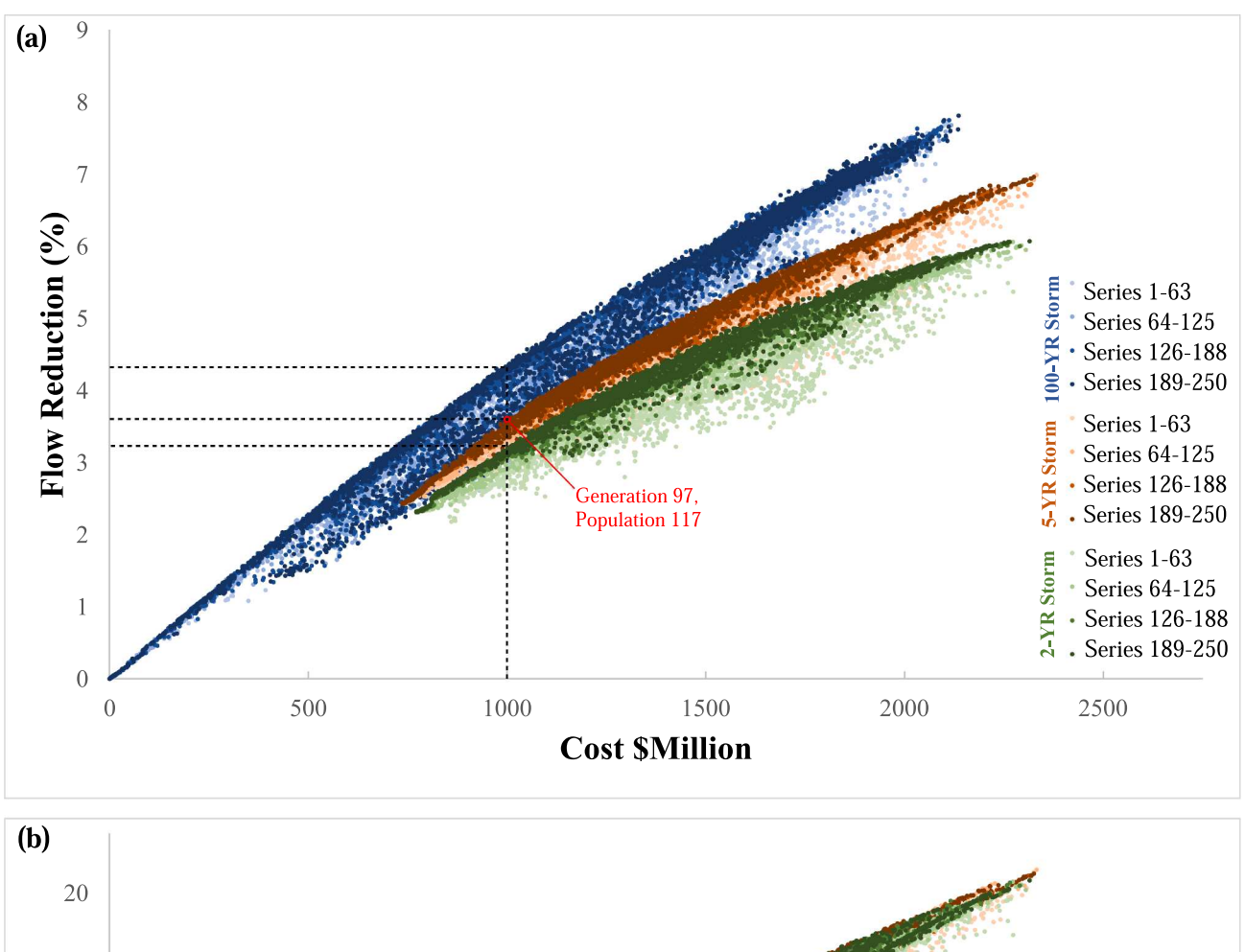
$$G_{e} = 1 - \sum_{i=0}^{m} (X_{i} - X_{(i-1)}) (Y_{i} - Y_{(i-1)}),$$
(10)

where Y_i is the y-axis value on the Lorenz curve, X_i is the x-axis value on the Lorenz curve (**Eq. 9a** is the X_i value for the hydrologic efficiency indicator, **Eq. 9b** is the X_i value for the environmental efficiency, and **Eq. 9c** is the X_i value for the social deprivation indicator), A_i is the area of each subcatchment i, with total subcatchments m, and G_e is the Gini coefficient corresponding to composite evaluation indices e = runoff volume efficiency, pollutant load efficiency, or social equity distribution. X_i and Y_i are plotted on the Lorenz curve by sorting Y_i in ascending order, where X_0 and Y_0 each equal 0.

Finally, the composite optimization objective is represented by:

Optimization Objective:
$$\min\left(\frac{\sum_{e=1}^{E} G_e}{E}\right)$$
, (11)

where G_e is the multi-functional Gini coefficient for each indicator, e,



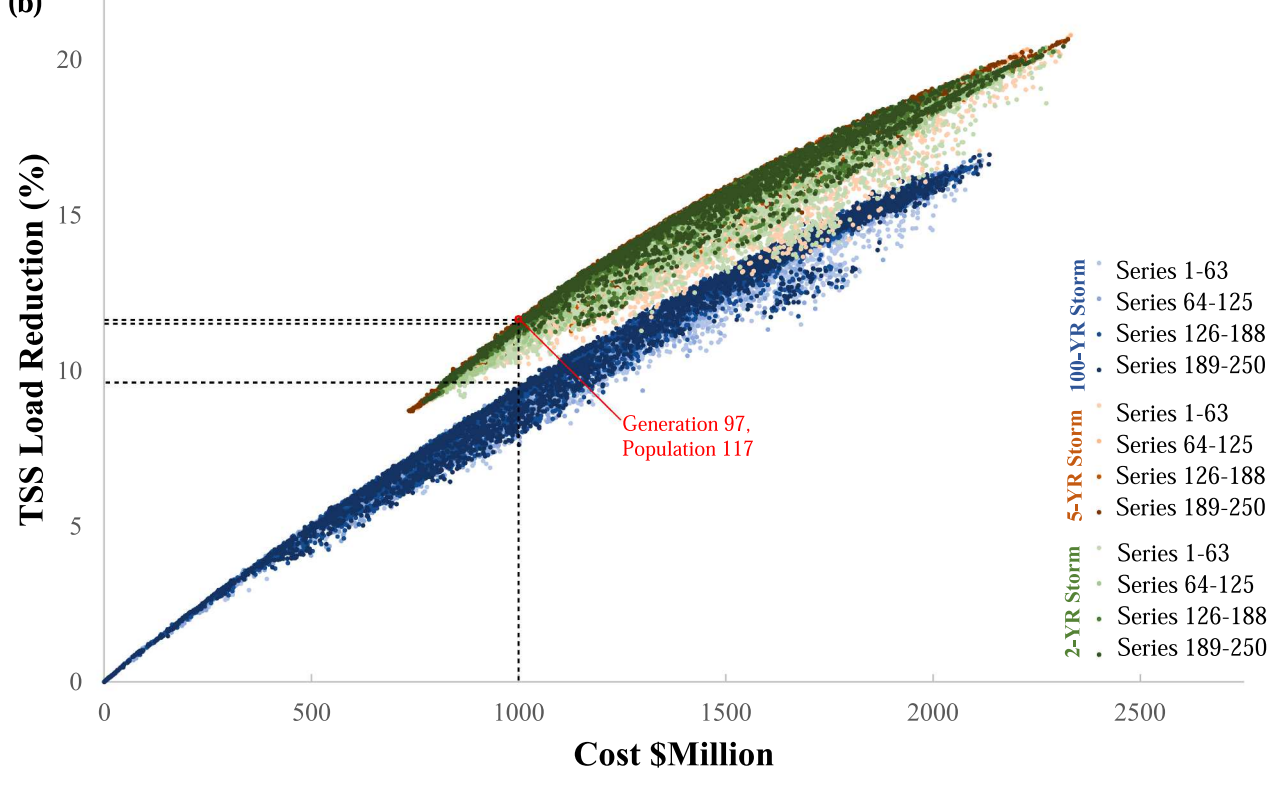


Fig. 4. Pareto front curves from the SWMM-based WOB optimization for 2-YR, 5-YR, and 100-YR design storms, represented by (a) flow reduction as a function of cost-efficiency and (b) pollutant load reduction as a function of cost-efficiency.

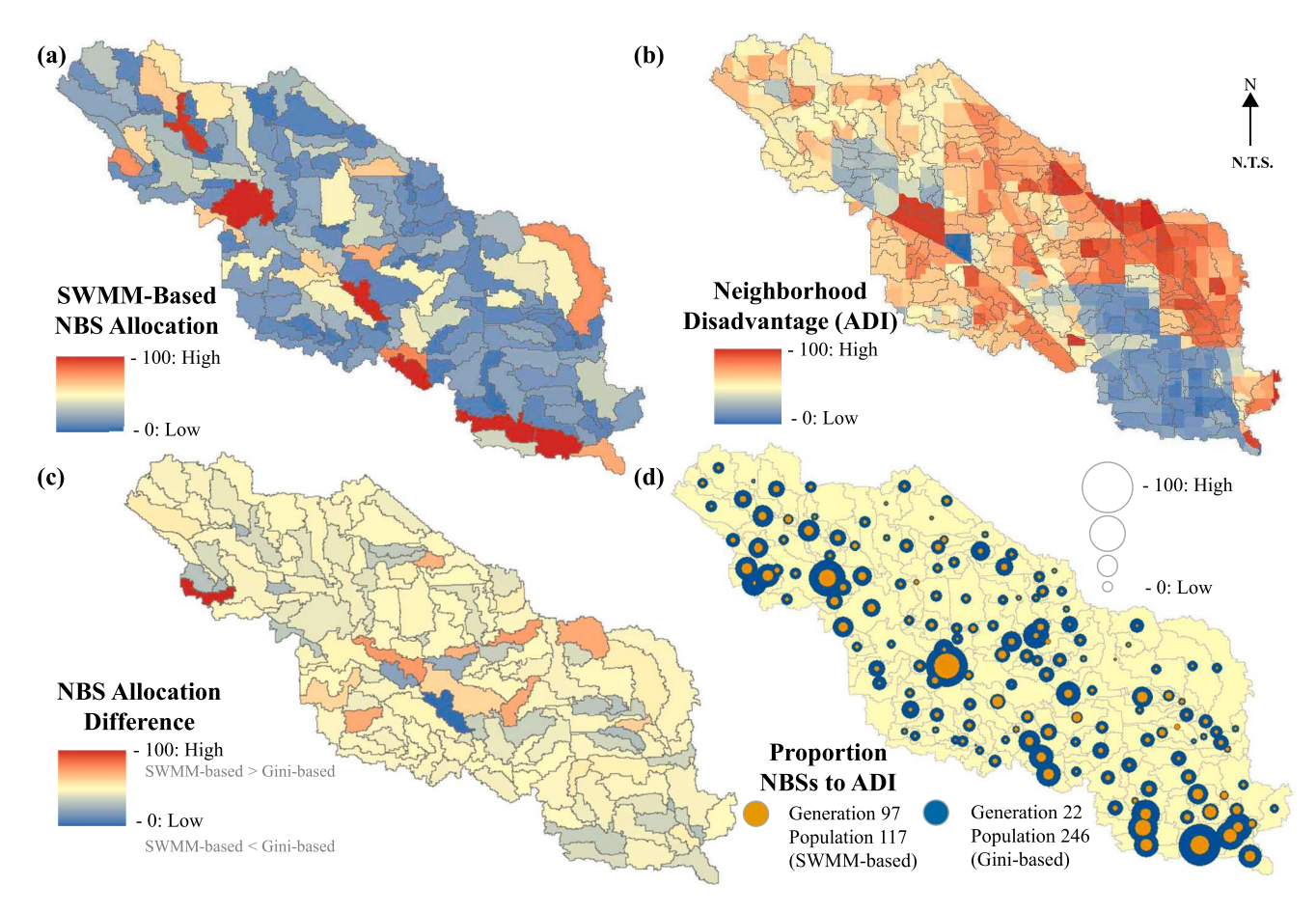


Fig. 5. Comparison of spatial distribution in the WOB watershed for the 5-YR storm per (a) NBS allocation according to optimal hydro-environmental efficiency (Generation 97, Population 117), (b) areas of neighborhood disadvantage, represented by the Area Deprivation Index (ADI), (c) difference between NBS allocation for SWMM-based optimization (Generation 97, Population 117) versus Gini-based optimization (Generation 22, Population 246), and (d) weighted proportion of NBS allocation within each subcatchment compared to ADI deprivation metrics.

over the total number of indicators E.

In summary, the following steps are applied to calculate the composite Gini index for amalgamating a series of NBS efficiency indicators according to both social well-being and hydro-environmental performance:

- Select a set of potential NBS allocation scenarios according to hydroenvironmental, SWMM-based modeling,
- 2. Calculate Lorenz curve values for each efficiency indicator (hydrologic, environmental, and social) and unique NBS scenario,
- 3. Plot the Lorenz curves and calculate the individual Gini indices,
- 4. Aggregate the objective functions and compare Lorenz curves according to the multi-criteria Gini coefficient, and
- 5. Minimize the optimization objective for the composite Gini coefficient to identify the most spatially-balanced distribution of social equality (i.e., NBS placement in areas of highest health deprivation) and hydro-environmental efficiency (i.e., NBS placement in areas of maximum runoff volume and pollutant load mitigation relative to cost).

3. Results and discussion

3.1. Hydro-environmental optimization

The 2-, 5-, and 100-year rainfall events were chosen as representative design storms for demonstrating the SWMM-based optimization of the WOB model, as demonstrated in Fig. 4. An example of planning for NBS expenditure of \$1,000 M is shown in the dashed lines where the optimal

Pareto front results in a flow reduction of 3.22%, 3.62%, and 4.37% and a TSS pollutant load reduction 11.69%, 11.65%, and 9.55% of for the 2-, 5-, and 100-year design storms, respectively. The cost-effectiveness curves (i.e., the Pareto fronts) suggest there exists a largely linear relationship between the level of NBS implementation and TSS pollutant load reduction between the 2-year and 5-year design storms. As noted in Fig. 4, the runoff volume and pollutant load efficiencies are inverted relative to design storm intensity. Higher cost-expenditures are associated with a greater number of NBS features for mitigating larger volumes of rainfall-runoff. Since pollutant loading concentrations are a function of land use, the percent-change in wash off is not significantly impacted by rainfall values. Consequently, the cost-efficiency for pollutant load reduction decreases as the design storm intensity (and thus NBS magnitude) increases. [Note: The GreenPlan-IT tool presents optimization results in monetary units of \$-million, which were maintained for purposes of this case study.]

The cost-effectiveness curves in Fig. 4 inform which Generation and Population models provide the most efficient hydro-environmental outcomes from the \sim 25,000 scenarios that were simulated in SWMM. Decision-makers can use these results to determine optimal NBS planning according to target expenditures. By assessing the far-right portion of the Pareto front, stakeholders may identify at which point further investment in NBS features yield no additional improvement in hydro-environmental goals. As such, hydrologic and environmental goals may be compared and contrasted between scenarios as a function of cost distribution and intensity of design storm metrics (SFEI, 2020). For example, if decision-makers had a goal of reducing the 100-YR runoff by 5% (equating to a total cost of \$1,187 M on the Pareto front curve in

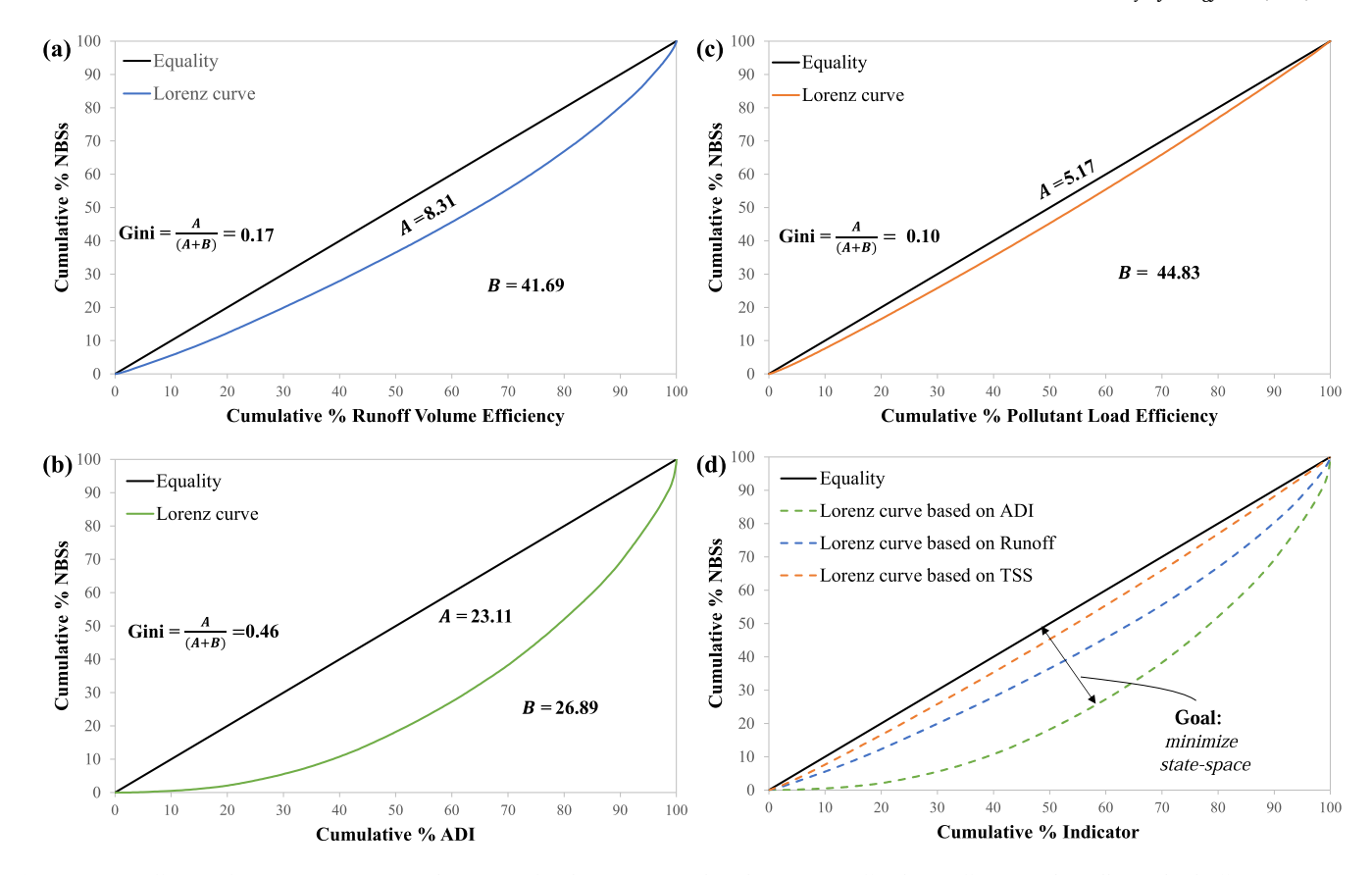


Fig. 6. Gini coefficients for Generation 97, Population 117 for the 5-YR storm based on (a) runoff volume efficiency, (b) pollutant load efficiency, (c) Area Deprivation Index, and (d) cumulative indicators.

Fig. 4a), stakeholders could quickly visualize the flow reduction efficiency for additional design storms and the tradeoffs associated with pollutant load abatement at this cost point.

To demonstrate how such optimization outputs may be combined with the multi-objective Gini coefficient, the 5-YR storm event with \$1,000 M expenditure was chosen for further investigation. In the SWMM-based approach, Generation 97, Population 117 produced the most optimal NBS allocation scenario according to hydro-environmental efficiency (i.e., 3.45% runoff volume reduction and 11.15% pollutant load reduction). In comparing the spatial distribution of NBSs from this model with the areas of highest social deprivation in the WOB watershed (Fig. 5a-b), we may note how sole reliance upon hydro-environmental characteristics for NBS planning could result in a missed opportunity to address potential social co-benefits from enhanced urban greening. As such, the multi-objective Gini coefficient is explored in the following section to refine the NBS optimization results.

3.2. Gini-based optimization

By plotting the Lorenz curves for the SWMM-based optimization model (Generation 97, Population 117) in Fig. 6, the individual Gini indices according to hydrologic efficiency, pollutant load efficiency, and social equity were calculated as 0.17, 0.10, and 0.46, respectively. A Gini coefficient less than or equal to 0.4 is commonly used as a threshold denoting fair distribution between the indicators on the x- and y-axes of the Lorenz curve (Groves-Kirkby et al., 2009; Sadras and Bongiovanni, 2004). Such results suggest a greater equity in NBS allocation on the basis of hydrodynamics compared with social characteristics. The large area between the Lorenz curve and the line of equality in Fig. 6b reveals poor allocation fairness corresponding to spatial distribution of neighborhood deprivation (i.e., the ADI index). As such, the framework presented here suggests amalgamating each of the individual Gini indices

 (G_i) to achieve a minimal composite Gini (G_e) toward a more equitable distribution of all evaluation indicators.

A sample set of outputs from the SWMM-based optimization was selected to demonstrate how the principal allocation scheme may shift when the multi-objective Gini coefficient is applied. As shown in Fig. 7 and summarized in Table 1, a cohort of 10 additional NBS planning scenarios were evaluated on the basis of the Gini coefficient for hydrologic, environmental, and social indicators. The construction of multiobjective Lorenz curves is demonstrated as the plotting of cumulative NBS spatial allocation against cumulative evaluation indicators, allowing for rapid comparison across planning scenarios. A larger area below the Lorenz curve suggests that the stormwater and social benefits are more variable within the planning paradigm, while a smaller area under the curve indicates a more uniform distribution of spatial planning for achieving multiple objectives. By comparing the width of the Lorenz curves and minimizing the composite Gini coefficient between these scenarios, the greatest distribution of equality occurs in planning scenario Generation 22, Population 246 ($G_e = 0.229$). The Gini-based plan provides a more equal distribution of overall benefits in comparison to the SWMM-based optimization model, Generation 97, Population 117 ($G_e = 0.243$), despite a similar investment in financial resources.

While the improvement in the composite Gini coefficient may appear modest, a detailed comparison between the optimization frameworks reveals a significant difference of NBS allocation in areas of greatest social need (i.e., high ADI score). As summarized in Table 2, the SWMM-based model only addresses 16.84% of the socially deprived areas when NBS features are sited for optimal hydro-environmental performance. By altering the composition of NBS features throughout the watershed, the Gini-based plan addresses 35.32% of the weighted ADI score within each subcatchment, while maintaining similar runoff and pollutant load reductions.

This difference in social-equity is further demonstrated in Fig. 5c-d,

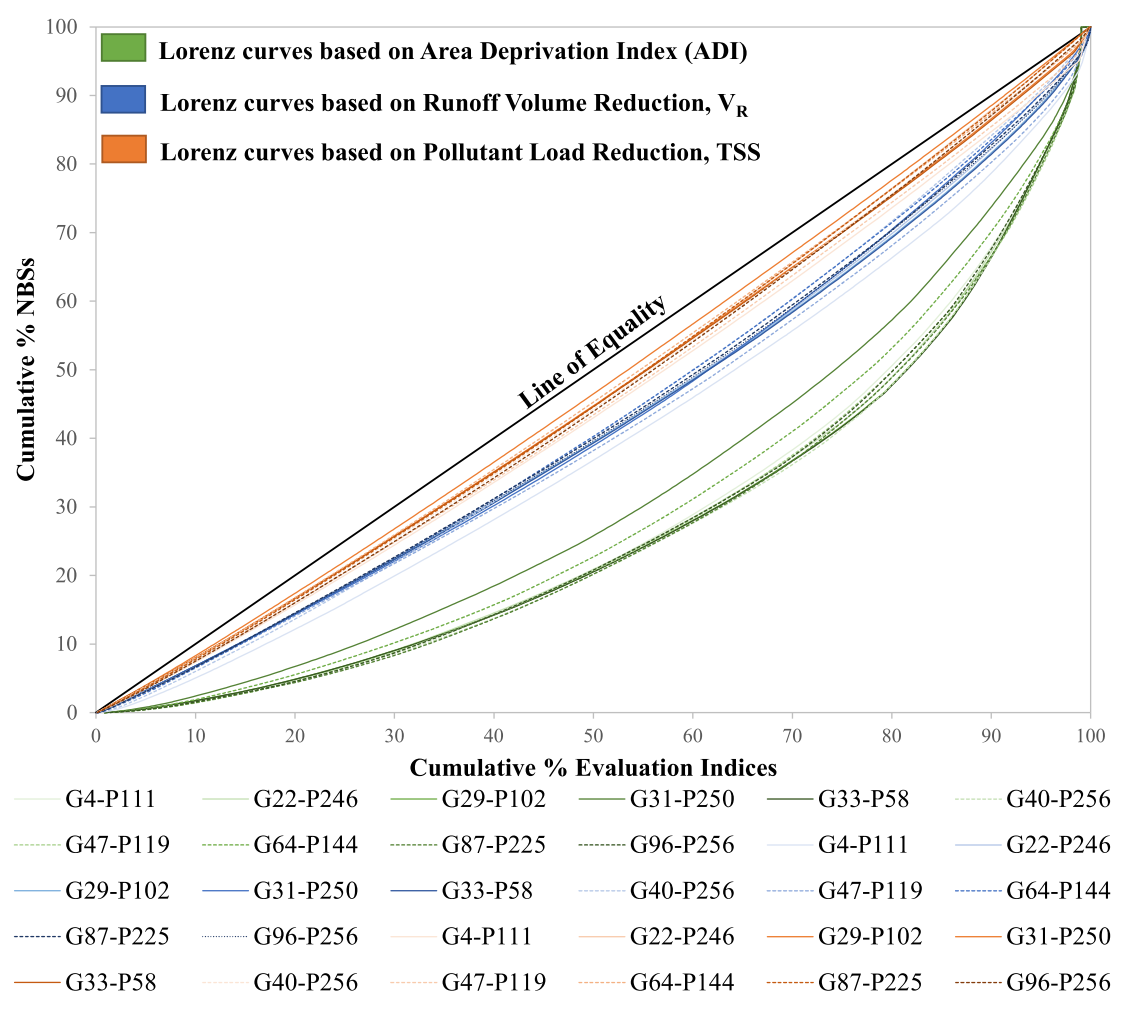


Fig. 7. Select cohort of 10 Lorenz curves from the 5-YR, ~\$1,000 M SWMM-based optimization, where G represents Generation (1–100), and P represents Population (1–250).

 $\textbf{Table 1} \\ \textbf{Select cohort of multi-objective Gini coefficients for the 5-YR, \sim1,000 M White Oak Bayou case study. }$

	G4 P111	G22 P246	G29 P102	G31 P250	G33 P58	G40 P256	G47 P119	G64 P144	G87 P225	G96 P256	G97 P117
G_{ADI}	0.436	0.443	0.448	0.442	0.449	0.455	0.444	0.482	0.452	0.442	0.460
G_{VR}	0.210	0.157	0.161	0.158	0.163	0.146	0.179	0.178	0.150	0.155	0.170
G_{TSS}	0.108	0.072	0.078	0.074	0.080	0.081	0.097	0.112	0.073	0.086	0.100
G _e	0.251	0.224	0.229	0.225	0.231	0.333	0.240	0.256	0.225	0.228	0.243

Table 2Comparison of SWMM-based (Generation 97, Population 117) optimal NBS plan versus the Gini-based (Generation 22, Population 246) allocation scheme for the White Oak Bayou, 5-YR storm event.

	G97 P117	G22 P246	
Cost (\$M)	\$1006	\$1000	
Runoff Volume Reduction	3.45%	3.38%	
Pollutant Load Reduction	11.15%	11.28%	
No. Bioretention Cells	168,459	189,385	
No. Porous Pavements	8,705	7,772	
No. Tree Boxes	239,001	154,824	
% ADI Addressed by NBSs	16.84%	35.32%	

where the SWMM-based and Gini-based models are compared spatially according to total NBS allocation and the corresponding proportion of NBS features to ADI deprivation. The holistic distribution of NBS cobenefits is shown in Fig. 8, where the pie charts represent the weighted efficiency achieved in each subcatchment according to hydrologic (blue), environmental (orange), and social (green) aspects. As observed in Fig. 8a, the SWMM-based model (Generation 97, Population 117) exhibits a high proportion of blue and orange areas throughout the WOB watershed, highlighting prioritization of hydro-environmental performance. Conversely, Fig. 8b (Generation 22, Population 246) contains a greater proportion of green areas, thereby revealing a greater influence of NBS allocation within socially vulnerable subcatchments. The primary reason for this disparity is that areas prone to flooding and environmental issues are not always spatially proportional to areas of highest social deprivation. As such, reliance upon a "worst-first" approach to NBS planning through the lens of hydro-dynamic modeling may result in non-optimal allocation for addressing the many societal

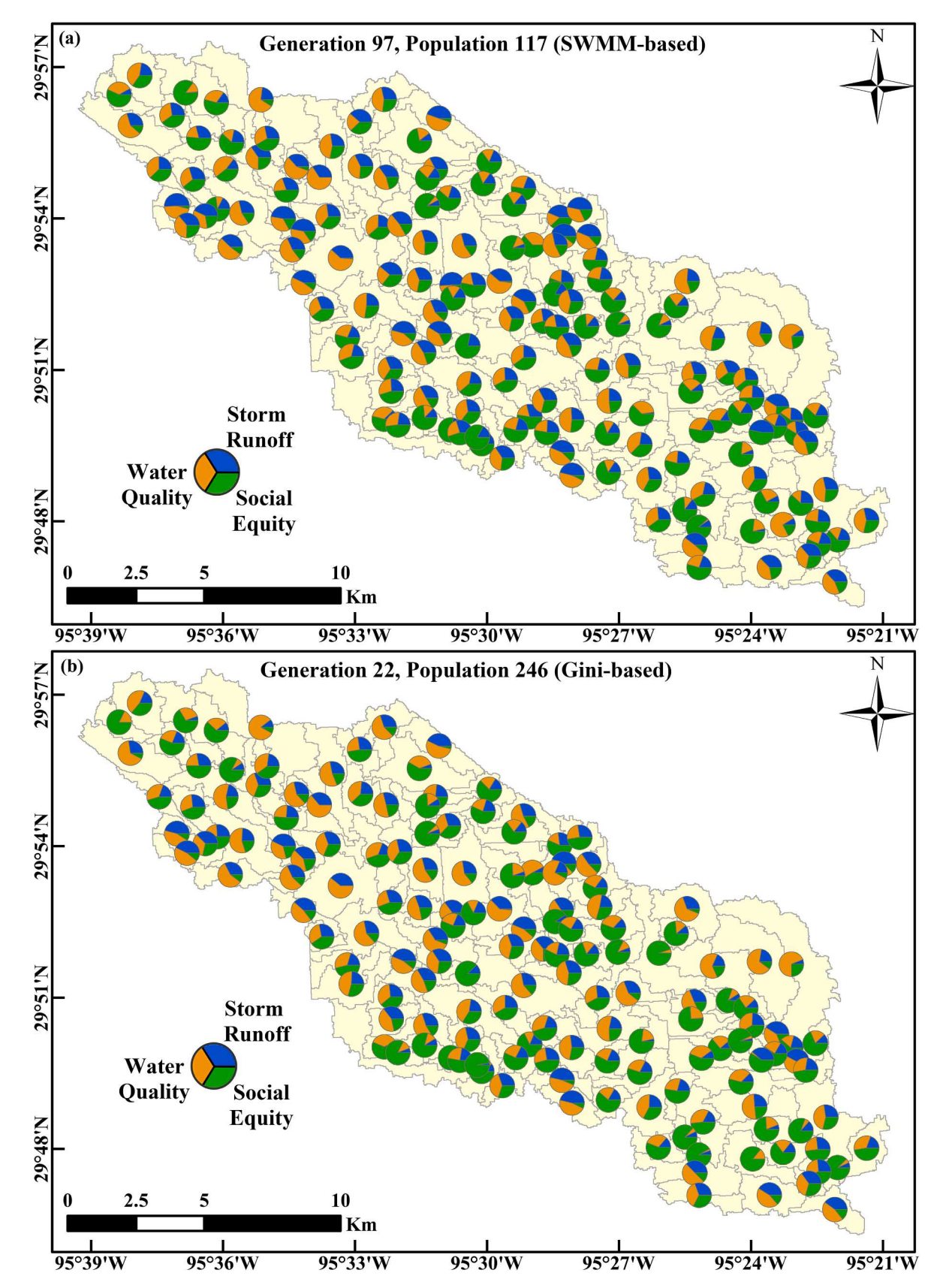


Fig. 8. Proportional representation of evaluation indicator efficiencies for (a) SWMM-based optimization model, and (b) Gini-based optimization model.

benefits provided by NBS solutions.

4. Limitations

It should be noted that the Gini coefficient is sensitive to outliers by its nature. As the Gini is a summary statistic, information may be lost when disparate datasets are combined, and an extreme value in one region of the graph can greatly impact the overall results. In other words, by converting all data along the Lorenz curve to a single number, disparate planning scenarios may result in a similar Gini coefficient (De Maio, 2007). As the Gini coefficient's sensitivity is related to the survey sample size and spatial resolution (Boyce et al., 2016; Fabrizi and Trivisano, 2016; Giorgi and Gigliarano, 2017), this study attempted to overcome such limitations by choosing a high-resolution measure of national social inequality (i.e., the ADI) and a robust measure of hydrologic performance according to detailed SWMM modeling. While outside the scope of this study, comparison of the spatial Gini coefficient to other measures of inequality and their sensitivity to outliers, of which many are presented throughout the literature (e.g., Boyce et al., 2016; Cobham and Sumner, 2013; Cowell and Flachaire, 2002; Sangüesa et al., 2018), is a worthwhile avenue of future research in amalgamating social inequality with environmental performance.

5. Conclusion

In the age of the Anthropocene, where hydrologic, environmental, and social processes are being influenced and altered by human patterns, NBSs serve as a prime foundation for exploring linkages between quality-of-life goals and water challenges. NBS design is a function of rapid urban development, social wellbeing, and a scarcity of resources for addressing hydro-meteorological challenges. As such, proper codevelopment of NBS plans can and should account for the multifunctional components involved in all of these processes for optimal impact. To amalgamate such inter-woven goals, decision-makers seek the ability to identify priority planning areas that guide equitable investment (Marchese et al., 2018). In considering the rising popularity of urban green infrastructure, we are presented with an opportunity to recast how decision-making operates in order to maximize the numerous co-benefits associated with NBSs.

As such, this study demonstrates how real-world social and hydroenvironmental complexities may be amalgamated using a novel application of the area Gini coefficient for actionable science. The Gini index is a straightforward calculation that could be used to merge holistic benefits using simple algebra. Since the coefficient of derivation under the Lorenz curve is calculated as a standard deviation, variation is relative, and thus invariant to changes in spatial scale. In other words, the Gini index provides a transparent measurement tool to describe the summary of impact fractions for multi-objective planning at cascading scales (Lee, 1997). By solely relying on hydro-environmental modeling, the relative benefits addressed by NBS solutions are limited and are not able to be optimized according to unique properties of socioeconomics and human health. This study is the first known attempt to incorporate NBS synergies and tradeoffs between hydrology, social health deprivation, environmental quality, and cost efficiency into a single framework using the dimensionless Gini coefficient.

The White Oak Bayou case study investigated how social equity and watershed dynamics propagate throughout the NBS system according to ~25,000 SWMM model runs. A comparison between traditional SWMM-based optimization and the proposed Gini-based framework revealed how the spatial allocation of NBSs within the watershed may be structured to address significantly more areas of social health deprivation while achieving similar hydro-environmental performance and cost-efficiency. The case study comparison revealed runoff volume reductions of 3.45% and 3.38%, pollutant load reductions of 11.15% and 11.28%, and ADI mitigation metrics of 16.84% and 35.32% for the SWMM-based and the Gini-based approaches, respectively, using similar

cost expenditures. By constructing the optimization framework with interdisciplinary elements, this study strengthened the planning capabilities associated with overlapping social and hydro-dynamic processes and patterns.

By approaching the system as a linkage of spatial properties, this study highlighted synergies associated with multiple human-water objectives, thereby reducing the potential for systemic underperformance (Marchese et al., 2018). Moreover, by integrating various epistemologies, this analytical approach serves as a representation of complex landscape functionalities and their unique interactions. As we continue to have increasing access to high-resolution datasets, the spatial Gini coefficient maximizes our understanding of local risks and benefits to answer challenging questions associated with multi-functional planning. The practical implications of this study will enhance the userfriendliness of NBS planning in an intuitive manner while merging well-established hydrological methodologies with social co-benefits (Kuller et al., 2017). When we are better able to connect the dots between social constructs, environmental processes, and the hydrological cycle, which are all complex processes that operate cohesively amongst one another, we can establish optimal patterns within the seemingly chaotic network of human-water phenomena. In a world with increasing socio-environmental stressors and finite resources, this research will improve public policy interventions by providing the knowledge necessary for identifying, quantifying, and linking complex interactions of NBS functions toward sound decision-making.

Declaration of Competing Interest

The authors declare that they have no known competing financial interests or personal relationships that could have appeared to influence the work reported in this paper.

Acknowledgements

The author thanks the efforts provided by Dr. Tan Zi of the San Francisco Estuary Institute (SFEI) for troubleshooting the GreenPlan-IT optimization tool to allow application to a large regional watershed in Houston, TX, USA.

Appendix A. Supplementary data

Supplementary data to this article can be found online at $\frac{https:}{doi.}$ org/10.1016/j.hydroa.2022.100127.

References

Addala, A., Auzanneau, M., Miller, K., Maier, W., Foster, N., Kapellen, T., Walker, A., Rosenbauer, J., Maahs, D.M., Holl, R.W., 2021. A decade of disparities in diabetes technology use and HBA1c in pediatric type 1 diabetes: A transatlantic comparison. Diabetes Care 44. https://doi.org/10.2337/dc20-0257.

Alamdari, N., Sample, D.J., 2019. A multiobjective simulation-optimization tool for assisting in urban watershed restoration planning. J. Clean. Prod. 213, 251–261.

Astell-Burt, T., Feng, X., 2021. Urban green space, tree canopy and prevention of cardiometabolic diseases: A multilevel longitudinal study of 46 786 Australians. Int. J. Epidemiol. 49 https://doi.org/10.1093/IJE/DYZ239.

Barrett, D., 2019. NOAA Atlas 14 PCPM IDF Curves Update.

Bernagros, J.T., Pankani, D., Struck, S.D., Deerhake, M.E., 2021. Estimating regionalized planning costs of green infrastructure and low-impact development stormwater management practices: updates to the US Environmental Protection Agency's National Stormwater Calculator. J. Sustain. Water Built Environ. 7 (2), 04020021.

Boano, F., Caruso, A., Costamagna, E., Ridolfi, L., Fiore, S., Demichelis, F., Galvão, A., Pisoeiro, J., Rizzo, A., Masi, F., 2020. A review of nature-based solutions for greywater treatment: Applications, hydraulic design, and environmental benefits. Sci. Total Environ. 711, 134731.

Boyce, J.K., Zwickl, K., Ash, M., 2016. Measuring environmental inequality. Ecol. Econ. 124, 114–123.

Branas, C.C., Cheney, R.A., MacDonald, J.M., Tam, V.W., Jackson, T.D., Ten Havey, T.R., 2011. A difference-in-differences analysis of health, safety, and greening vacant urban space. Am. J. Epidemiol. 174. 10.1093/aje/kwr273.

C40, 2017. Benefits of Climate Action - Houston: Benefits of the White Oak Bayou Greenway.

- Castro, C.V., Maidment, D.R., 2020. GIS preprocessing for rapid initialization of HEC-HMS hydrological basin models using web-based data services. Environ. Model. Softw. 130, 104732.
- Chamberlain, A.M., Finney Rutten, L.J., Wilson, P.M., Fan, C., Boyd, C.M., Jacobson, D. J., Rocca, W.A., St Sauver, J.L., 2020. Neighborhood socioeconomic disadvantage is associated with multimorbidity in a geographically-defined community. BMC Public Health 20. https://doi.org/10.1186/s12889-019-8123-0.
- Chen, C.W., Shubinski, R.P., 1971. Computer Simulation of Urban Storm Water Runoff. J. Hydraul. Div. 97 (2), 289–301.
- CHI, 2014. PCSWMM Support: Transect creator.
- Cho, J.H., Lee, J.H., 2014. Multi-objective waste load allocation model for optimizing waste load abatement and inequality among waste dischargers. Water. Air. Soil Pollut. 225 https://doi.org/10.1007/s11270-014-1892-2.
- Choi, K.-S., Ball, J.E., 2002. Parameter estimation for urban runoff modelling. Urban Water 4 (1), 31–41.
- Clary, J., Leisenring, M., Strecker, E., 2020. International Stormwater BMP Database: 2020 Summary Statistics.
- CNT, 2009. National green values calculator methodology. Cent. Neighborhood Technol Sustainabl.
- Cobham, A., Sumner, A., 2013. Putting the gini back in the bottle? 'The Palma' As a policy-relevant measure of inequality. J. Chem. Inf Model 53.
- COH, 2021. City of Houston Data Hub.
- COH, 2019a. Infrastructure Design Manual 2019, Section 9.2.01.B.1, Design Rainfall Events.
- COH, 2019b. City of Houston Design Manual: Chapter 9, Stormwater Design Requirements, Section 9.15.
- Cowell, F., Flachaire, E., 2002. Sensitivity of Inequality Measures to Extreme Values. LSE STICERD.
- Crompton, J.L., 2012. Estimates of the Economic Benefits Accruing From and Expansion of Houston's Bayou Greenway Network.
- De Maio, F.G., 2007. Income inequality measures. J. Epidemiol. Community Health. 61 (10), 849–852.
- de Vries, S., Verheij, R.A., Groenewegen, P.P., Spreeuwenberg, P., 2003. Natural environments - Healthy environments? An exploratory analysis of the relationship between greenspace and health. Environ. Plan. A 35 (10), 1717–1731.
- Deb, K., Pratap, A., Agarwal, S., Meyarivan, T., 2002. A fast and elitist multiobjective genetic algorithm: NSGA-II. IEEE Trans. Evol. Comput. 6 (2), 182–197.
- Despart, Z., 2019. Harris County approves "worst-first" priority model for flood bond projects.
- Druckman, A., Jackson, T., 2008. Measuring resource inequalities: The concepts and methodology for an area-based Gini coefficient. Ecol. Econ. 65 (2), 242–252.
- Du, E., Cai, X., Wu, F., Foster, T., Zheng, C., 2021. Exploring the impacts of the inequality of water permit allocation and farmers' behaviors on the performance of an agricultural water market. J. Hydrol. 599, 126303.
- Fabrizi, E., Trivisano, C., 2016. Small area estimation of the Gini concentration coefficient. Comput. Stat. Data Anal. 99, 223–234.
- Flanagan, B.E., Gregory, E.W., Hallisey, E.J., Heitgerd, J.L., Lewis, B., 2020. A Social Vulnerability Index for Disaster Management. J. Homel. Secur. Emerg. Manag. 8 https://doi.org/10.2202/1547-7355.1792.
- Frantzeskaki, N., McPhearson, T., Collier, M.J., Kendal, D., Bulkeley, H., Dumitru, A., Walsh, C., Noble, K., Van Wyk, E., Ordóñez, C., Oke, C., Pintér, L., 2019. Naturebased solutions for urban climate change adaptation: Linking science, policy, and practice communities for evidence-based decision-making. Bioscience 69. 10.1093/ biosci/biz042.
- Fuertes, E., Markevych, I., von Berg, A., Bauer, C.-P., Berdel, D., Koletzko, S., Sugiri, D., Heinrich, J., 2014. Greenness and allergies: Evidence of differential associations in two areas in Germany. J. Epidemiol. Community Health 68 (8), 787–790.
- Gascon, M., Triguero-Mas, M., Martínez, D., Dadvand, P., Rojas-Rueda, D., Plasència, A., Nieuwenhuijsen, M.J., 2016. Residential green spaces and mortality: A systematic review. Environ. Int. 86, 60–67.
- Giacomoni, M.H., Joseph, J., 2017. Multi-Objective Evolutionary Optimization and Monte Carlo Simulation for Placement of Low Impact Development in the Catchment Scale. J. Water Resour. Plan. Manag. 143 (9), 04017053.
- Gini, C.W., 1912. Variability and Mutability, contribution to the study of statistical distributions and relations. Stud. Econ. della Stud. Econ. della R. Univ Cagliari.
- Giorgi, G.M., Gigliarano, C., 2017. The gini concentration index: a review of the inference literature. J. Econ. Surv. $31\ (4), 1130-1148$.
- GLA, 2018. Green Infrastructure Focus Map: Briefing 1. London.
- Groves-Kirkby, C.J., Denman, A.R., Phillips, P.S., 2009. Lorenz Curve and Gini Coefficient: Novel tools for analysing seasonal variation of environmental radon gas. J. Environ. Manage. 90 (8), 2480–2487.
- Hamouz, V., Møller-Pedersen, P., Muthanna, T.M., 2020. Modelling runoff reduction through implementation of green and grey roofs in urban catchments using PCSWMM. Urban Water J. 17 (9), 813–826.
- HCFCD, 2021. Harris County Flood Warning System.
- Hcfcd, 2019. Model and map management system (M3). Harris Cty, Flood Control Dist. Heckert, M., Rosan, C.D., 2016. Developing a green infrastructure equity index to promote equity planning. Urban For. Urban Green. 19, 263–270.
- Heerink, N., Mulatu, A., Bulte, E., 2001. Income inequality and the environment: Aggregation bias in environmental Kuznets curves. Ecol. Econ. 38 (3), 359–367.
- Hirshberg, E.L., Wilson, E.L., Stanfield, V., Kuttler, K.G., Majercik, S., Beesley, S.J., Orme, J., Hopkins, R.O., Brown, S.M., 2019. Impact of critical illness on resource utilization: A comparison of use in the year before and after ICU admission. Crit. Care Med. 47 (11), 1497–1504.

- Hu, Z., Chen, Y., Yao, L., Wei, C., Li, C., 2016. Optimal allocation of regional water resources: From a perspective of equity-efficiency tradeoff. Resour. Conserv. Recycl. 109, 102–113.
- Huang, L., Li, X., Fang, H., Yin, D., Si, Y., Wei, J., Liu, J., Hu, X., Zhang, L.i., 2019. Balancing social, economic and ecological benefits of reservoir operation during the flood season: A case study of the Three Gorges Project, China. J. Hydrol. 572, 422–434.
- Ingraham, N.E., Purcell, L.N., Karam, B.S., Dudley, R.A., Usher, M.G., Warlick, C.A., Allen, M.L., Melton, G.B., Charles, A., Tignanelli, C.J., 2021. Racial and Ethnic Disparities in Hospital Admissions from COVID-19: Determining the Impact of Neighborhood Deprivation and Primary Language. J. Gen. Intern. Med. https://doi. org/10.1007/s11606-021-06790-w.
- Jacobson, A., Milman, A.D., Kammen, D.M., 2005. Letting the (energy) Gini out of the bottle: Lorenz curves of cumulative electricity consumption and Gini coefficients as metrics of energy distribution and equity. Energy Policy 33 (14), 1825–1832.
- James, W., 2003. Rules for responsible modeling.
- Jarden, K.M., Jefferson, A.J., Grieser, J.M., 2016. Assessing the effects of catchment-scale urban green infrastructure retrofits on hydrograph characteristics. Hydrol. Process. 30 (10), 1536–1550.
- Jato-Espino, D., Charlesworth, S., Bayon, J., Warwick, F., 2016. Rainfall-runoff simulations to assess the potential of suds for mitigating flooding in highly urbanized catchments. Int. J. Environ. Res. Public Health 13 (1), 149.
- Jessup, K., Parker, S.S., Randall, J.M., Cohen, B.S., Roderick-Jones, R., Ganguly, S., Sourial, J., 2021. Planting Stormwater Solutions: A methodology for siting naturebased solutions for pollution capture, habitat enhancement, and multiple health benefits. Urban For. Urban Green. 64, 127300.
- Josa, I., Aguado, A., 2020. Measuring unidimensional inequality: practical framework for the choice of an appropriate measure. Soc. Indic. Res. 149 (2), 541–570.
- Kabisch, N., Frantzeskaki, N., Pauleit, S., Naumann, S., Davis, M., Artmann, M., Haase, D., Knapp, S., Korn, H., Stadler, J., Zaunberger, K., Bonn, A., 2016. Nature-based solutions to climate change mitigation and adaptation in urban areas: Perspectives on indicators, knowledge gaps, barriers, and opportunities for action. Ecol. Soc. 21 https://doi.org/10.5751/ES-08373-210239.
- Kaczynski, A.T., Henderson, K.A., 2007. Environmental correlates of physical activity: A review of evidence about parks and recreation. Leis. Sci. 29 (4), 315–354.
- Kandakoglu, A., Frini, A., Ben Amor, S., 2019. Multicriteria decision making for sustainable development: A systematic review. J. Multi-Criteria Decis. Anal. 26 (5-6). 202–251.
- Kind, A.J.H., Buckingham, W.R., 2018. Making Neighborhood-Disadvantage Metrics Accessible — The Neighborhood Atlas. N. Engl. J. Med. 378 (26), 2456–2458.
- Knighton, A.J., Savitz, L., Belnap, T., Stephenson, B., VanDerslice, J., 2016. Introduction of an Area Deprivation Index Measuring Patient Socio-economic Status in an Integrated Health System: Implications for Population Health. eGEMs (Generating Evid. Methods to Improv. patient outcomes) 4. 10.13063/2327-9214.1238.
- Krebs, G., Kokkonen, T., Valtanen, M., Koivusalo, H., Setälä, H., 2013. A high resolution application of a stormwater management model (SWMM) using genetic parameter optimization. Urban Water J. 10 (6), 394–410.
- Kuller, M., Bach, P.M., Ramirez-Lovering, D., Deletic, A., 2017. Framing water sensitive urban design as part of the urban form: A critical review of tools for best planning practice. Environ. Model. Softw. 96, 265–282.
- Kurani, S.S., McCoy, R.G., Lampman, M.A., Doubeni, C.A., Finney Rutten, L.J., Inselman, J.W., Giblon, R.E., Bunkers, K.S., Stroebel, R.J., Rushlow, D., Chawla, S.S., Shah, N.D., 2020. Association of neighborhood measures of social determinants of health with breast, cervical, and colorectal cancer screening rates in the US Midwest. JAMA Netw. open 3 (3), e200618.
- La Rosa, D., Pappalardo, V., 2020. Planning for spatial equity A performance based approach for sustainable urban drainage systems. Sustain. Cities Soc. 53, 101885.
- Lee, J.G., Selvakumar, A., Alvi, K., Riverson, J., Zhen, J.X., Shoemaker, L., Lai, F., hsiung,, 2012. A watershed-scale design optimization model for stormwater best management practices. Environ. Model. Softw. 37 https://doi.org/10.1016/j.envsoft.2012.04.011.
- Lee, W.-C., 1997. Characterizing exposure-disease association in human populations using the Lorenz curve and Gini index. Stat. Med. 16 (7), 729–739.
- Link, B.G., Phelan, J.o., 1995. Social conditions as fundamental causes of disease. J. Health Soc. Behav. 35, 80.
- Liu, L.i., Jensen, M.B., 2018. Green infrastructure for sustainable urban water management: Practices of five forerunner cities. Cities 74, 126–133.
- Liu, Y., Wang, C., Yu, Y., Chen, Y., Du, L., Qu, X., Peng, W., Zhang, M., Gui, C., 2019. Effect of urban stormwater road runoffof different land use types on an urban river in Shenzhen. China. Water (Switzerland) 11 (12), 2545.
- Loperfido, J.V., Noe, G.B., Jarnagin, S.T., Hogan, D.M., 2014. Effects of distributed and centralized stormwater best management practices and land cover on urban stream hydrology at the catchment scale. J. Hydrol. 519, 2584–2595.
- Luck, G.W., Smallbone, L.T., O'Brien, R., 2009. Socio-economics and vegetation change in urban ecosystems: Patterns in space and time. Ecosystems 12 (4), 604–620.
- Ludwig, J., Sanbonmatsu, L., Gennetian, L., Adam, E., Duncan, G.J., Katz, L.F., Kessler, R. C., Kling, J.R., Lindau, S.T., Whitaker, R.C., McDade, T.W., 2011. Neighborhoods, Obesity, and Diabetes A Randomized Social Experiment. N. Engl. J. Med. 365 (16), 1509–1519.
- Macro, K., Matott, L.S., Rabideau, A., Ghodsi, S.H., Zhu, Z., 2019. OSTRICH-SWMM: A new multi-objective optimization tool for green infrastructure planning with SWMM. Environ. Model. Softw. 113, 42–47.
- Mani, M., Bozorg-Haddad, O., Loáiciga, H.A., 2019. A new framework for the optimal management of urban runoff with low-impact development stormwater control measures considering service-performance reduction. J. Hydroinformatics 21 (5), 727–744.

- Marchese, D., Reynolds, E., Bates, M.E., Morgan, H., Clark, S.S., Linkov, I., 2018. Resilience and sustainability: Similarities and differences in environmental management applications. Sci. Total Environ. 613-614, 1275–1283.
- Martikainen, P., Mäki, N., Blomgren, J., 2004. The effects of area and individual social characteristics on suicide risk: A multilevel study of relative contribution and effect modification. Eur. J. Popul. 20 (4), 323–350.
- Meerow, S., Newell, J.P., 2017. Spatial planning for multifunctional green infrastructure: Growing resilience in Detroit. Landsc. Urban Plan. 159, 62–75.
- Mitchell, R., Popham, F., 2008. Effect of exposure to natural environment on health inequalities: an observational population study. Lancet 372 (9650), 1655–1660.
- Muleta, M.K., Boulos, P.F., 2007. Multiobjective optimization for optimal design of urban drainage systems. In: Restoring Our Natural Habitat - Proceedings of the 2007 World Environmental and Water Resources Congress. https://doi.org/10.1061/40927(243) 172
- Nkoy, F.L., Stone, B.L., Knighton, A.J., Fassl, B.A., Johnson, J.M., Maloney, C.G., Savitz, L.A., 2018. Neighborhood deprivation and childhood asthma outcomes. Accounting for Insurance Coverage. Hosp. Pediatr. 8 (2), 59–67.
- Oraei Zare, S., Saghafian, B., Shamsai, A., 2012. Multi-objective optimization for combined quality-quantity urban runoff control. Hydrol. Earth Syst. Sci. 16 (12), 4521, 4522.
- Perica, S., Pavlovic, S., Laurent, M. St., Trypaluk, C., Unruh, D., Wilhite, O., 2018. NOAA Atlas 14 Precipitation-Frequency Atlas of the United States Volume 11 Version 2.0: Texas.
- Pitt, R., Maestre, A., Clary, J., 2015. National Stormwater Quality Database (NSQD), Version 4.02 (2001-2015).
- Radinja, M., Comas, J., Corominas, L., Atanasova, N., 2019. Assessing stormwater control measures using modelling and a multi-criteria approach. J. Environ. Manage. 243, 257–268
- Raei, E., Reza Alizadeh, M., Reza Nikoo, M., Adamowski, J., 2019. Multi-objective decision-making for green infrastructure planning (LID-BMPs) in urban storm water management under uncertainty. J. Hydrol. 579, 124091.
- Rossi, L., Fankhauser, R., Chèvre, N., 2006. Water quality criteria for total suspended solids (TSS) in urban wet-weather discharges. Water Sci. Technol. 54. 10.2166/ wst.2006.623.
- Rossman, L.A., Huber, W.C., 2016. Storm Water Management Model User's Manual, United States Environment Protection Agency.
- Ruangpan, L., Vojinovic, Z., Di Sabatino, S., Leo, L.S., Capobianco, V., Oen, A.M.P., Mcclain, M.E., Lopez-Gunn, E., 2020. Nature-based solutions for hydrometeorological risk reduction: a state-of-the-art review of the research area. Nat. Hazards Earth Syst. Sci. 20 https://doi.org/10.5194/nhess-20-243-2020.
- Saboohi, Y., 2001. An evaluation of the impact of reducing energy subsidies on living expenses of households. Energy Policy 29 (3), 245–252.
- Sadras, V., Bongiovanni, R., 2004. Use of Lorenz curves and Gini coefficients to assess yield inequality within paddocks. F. Crop. Res. 90 (2-3), 303–310.
- Sangüesa, C., Pizarro, R., Ibañez, A., Pino, J., Rivera, D., García-Chevesich, P., Ingram, B., 2018. Spatial and temporal analysis of rainfall concentration using the Gini Index and PCI. Water (Switzerland) 10 (2), 112.
- Sarabi, S., Han, Q.i., Romme, A.G.L., de Vries, B., Valkenburg, R., den Ouden, E., 2020. Uptake and implementation of Nature-Based Solutions: An analysis of barriers using Interpretive Structural Modeling. J. Environ. Manage. 270, 110749.
- Schlossberg, M., 2003. GIS, the US census and neighbourhood scale analysis. Plan. Pract. Res. 18 (2-3), 213.
- SFEI, 2020. GreenPlan-IT Case Study: San Jose's Urban Villages, Chapter 3. SFEI, 2018. GreenPlanIT Optimization Tool User Manual.
- Singh, G.K., 2003. Area Deprivation and Widening Inequalities in US Mortality, 1969–1998. Am. J. Public Health 93 (7), 1137–1143

- Sipes, J.L. and Zeve, M.K., 2012. The Bayous of Houston.
- Sun, T., Zhang, H., Wang, Y., Meng, X., Wang, C., 2010. The application of environmental Gini coefficient (EGC) in allocating wastewater discharge permit: The case study of watershed total mass control in Tianjin. China. Resour. Conserv. Recycl. 54 (9), 601–608.
- Tao, T., Wang, J., Xin, K., Li, S., 2014. Multi-objective optimal layout of distributed storm-water detention. Int. J. Environ. Sci. Technol. 11 (5), 1473–1480.
- TNRIS, 2019. Harris County LiDAR 2018.
- UNEP, 2019. The UN Environment Programme and nature-based solutions.
- University of Wisconsin School of Medicine and Public, 2019. Area Deprivation Index. USDA, 1986. Urban Hydrology for Small Watersheds: TR-55.
- USGS, 2021. USGS 08074020 Whiteoak Bayou at Alabonson Rd. Houston, TX.
- USGS, 2021b. USGS 08074500 Whiteoak Bayou at Houston, TX.
- van den Berg, A.E., Maas, J., Verheij, R.A., Groenewegen, P.P., 2010. Green space as a buffer between stressful life events and health. Soc. Sci. Med. 70 (8), 1203–1210.
- van den Bosch, M., Ode Sang, Å., 2017. Urban natural environments as nature-based solutions for improved public health – A systematic review of reviews. Environ. Res. 158, 373–384.
- Vandermeulen, V., Verspecht, A., Vermeire, B., Van Huylenbroeck, G., Gellynck, X., 2011. The use of economic valuation to create public support for green infrastructure investments in urban areas. Landsc. Urban Plan. 103 (2), 198–206.
- Wamsler, C., Wickenberg, B., Hanson, H., Alkan Olsson, J., Stålhammar, S., Björn, H., Falck, H., Gerell, D., Oskarsson, T., Simonsson, E., Torffvit, F., Zelmerlow, F., 2020. Environmental and climate policy integration: Targeted strategies for overcoming barriers to nature-based solutions and climate change adaptation. J. Clean. Prod. 247, 119154.
- White, T.J., 2007. Sharing resources: The global distribution of the Ecological Footprint. Ecol. Econ. 64 (2), 402–410.
- Wolch, J.R., Byrne, J., Newell, J.P., 2014. Urban green space, public health, and environmental justice: The challenge of making cities "just green enough". Landsc. Urban Plan. 125, 234–244.
- Wong, S.M., Montalto, F.A., 2020. Exploring the long-term economic and social impact of green infrastructure in New York City. Water Resour. Res. 56 https://doi.org/ 10.1029/2019WR027008.
- Wu, J., Kauhanen, P.G., Hunt, J.A., Senn, D.B., Hale, T., McKee, L.J., 2019. Optimal Selection and Placement of Green Infrastructure in Urban Watersheds for PCB Control. J. Sustain. Water Built Environ. 5 (2), 04018019.
- Yan, D., Jia, Z., Xue, J., Sun, H., Gui, D., Liu, Y.i., Zeng, X., 2018. Inter-regional coordination to improve equality in the agricultural virtualwater trade. Sustain. 10 (12), 4561.
- Yang, L., Jin, S., Danielson, P., Homer, C., Gass, L., Bender, S.M., Case, A., Costello, C., Dewitz, J., Fry, J., Funk, M., Granneman, B., Liknes, G.C., Rigge, M., Xian, G., 2018. A new generation of the United States National Land Cover Database: Requirements, research priorities, design, and implementation strategies. ISPRS J. Photogramm. Remote Sens. 146. 108–123.
- Zellner, M., Massey, D., Minor, E., Gonzalez-Meler, M., 2016. Exploring the effects of green infrastructure placement on neighborhood-level flooding via spatially explicit simulations. Comput. Environ. Urban Syst. 59, 116–128.
- Zhang, D., Shen, J., Liu, P., Zhang, Q., Sun, F., 2020. Use of fuzzy analytic hierarchy process and environmental gini coefficient for allocation of regional flood drainage rights. Int. J. Environ. Res. Public Health 17 (6), 2063.
- Zhang, G., Hamlett, J.M., Reed, P., Tang, Y., 2013. Multi-Objective Optimization of Low Impact Development Designs in an Urbanizing Watershed. Open J. Optim. 02 (04), 95–108.

Contents lists available at ScienceDirect

Journal of Hydrology X

journal homepage: www.sciencedirect.com/journal/journal-of-hydrology-x





Corrigendum to "Optimizing nature-based solutions by combining social equity, hydro-environmental performance, and economic costs through a novel Gini coefficient" [J. Hydrol. 16 (2022) 100127]

C.V. Castro

Department of Civil Engineering, University of Illinois at Urbana-Champaign, Urbana, IL 61801, USA

The author would like to inform the addition of the below sentence in the Acknowledgement section,

"This material was based upon work supported by the National

Science Foundation under Award No. 2052598."

The author would like to apologise for any inconvenience caused.

DOI of original article: https://doi.org/10.1016/j.hydroa.2022.100127. *E-mail address*: cvcastro@illinois.edu.